

# Titanium Dioxide Coupled with Tungsten Trioxide and Titanium Dioxide Coupled with Molybdenum Trioxide Nanocomposite-Assisted Photocatalytic Inactivation of *Escherichia coli* in Direct Sunlight, Solar Simulator, and Visible Light

Florence Masese<sup>1,a\*</sup>, Shem O. Wandiga<sup>1</sup>, Vincent Madadi<sup>1</sup>, Damaris Mbui<sup>1</sup> & Stephen Ojwach<sup>2</sup>

<sup>1</sup>Department of Chemistry, P.O. Box 30197-00100, Nairobi, Kenya

<sup>2</sup>University of KwaZulu-Natal, School of Chemistry and Physics, Private bag X01, Scottsville 3209, South Africa.

<sup>a</sup>Email: [maseseflorence15@gmail.com](mailto:maseseflorence15@gmail.com)\*

## ARTICLE INFO

### Article History:

Received: April 2023

Accepted: December 2023

Available online: 25 July 2024

### Keywords:

Photocatalysis

semi-conductors

reactive oxygen species

*Escherichia coli*

## ABSTRACT

Photocatalysis may be considered as a possible alternative method in the elimination of *Escherichia coli* from domestic water. It has several advantages when compared with conventional methods, as it is non-toxic, utilizes energy from the sun and offers a green route that could be used to purify water polluted with *Escherichia coli*. The aim of the study was to investigate the effectiveness of the synthesized modified titanium dioxide photocatalyst in disinfecting *Escherichia coli* in domestic water under varied light intensities. *Escherichia coli* concentrations between 400 and 800 colony forming units per milliliter were used to investigate photocatalytic disinfection of the water containing *Escherichia coli*, under three different sources of light; visible light, natural sunlight and illumination from a solar simulator.

The two linked photocatalysts, titanium dioxide coupled with tungsten trioxide and titanium dioxide coupled with molybdenum trioxide were compared in disinfection studies to examine the impact of catalyst loading on disinfection rate. The synthesised photocatalysts were also characterised using the Energy Dispersive X-ray, Transmission Electron Microscopy, and Scanning Electron Microscope. The results showed that titanium dioxide coupled with tungsten trioxide was more successful in killing *Escherichia coli* bacteria compared to titanium dioxide coupled with molybdenum trioxide across all tested light sources: natural sunlight, visible light, and light from a solar simulator. After 120 minutes of irradiation using 1g/L of each catalyst, the results showed significant differences in inactivation efficiencies. Under natural sunlight, titanium dioxide coupled with tungsten trioxide achieved a high disinfection rate of 96%, whereas titanium dioxide coupled with molybdenum trioxide achieved 89%. A similar trend was observed under visible light, with efficiencies of 95% and 88% for titanium dioxide coupled with tungsten trioxide and titanium dioxide coupled with molybdenum trioxide respectively. When exposed to irradiation from a solar simulator, titanium dioxide coupled with tungsten trioxide performed better, with an efficiency of 92%, compared to 83% for titanium dioxide coupled with molybdenum trioxide. Experiments carried out without catalysts, served as blanks. These experimental results confirm that coupled titanium dioxide nanoparticles are effective and may be used in treating domestic water contaminated with *Escherichia coli*.

***Titanium Dioxide Coupled with Tungsten Trioxide and Titanium Dioxide Coupled with Molybdenum Trioxide Nanocomposite-Assisted Photocatalytic Inactivation of Escherichia coli in Direct Sunlight, Solar Simulator, and Visible Light***

## **1. Introduction**

Availability of potable freshwater continues to be a big challenge throughout the world. According to the World Health Organization's [24] factsheet on drinking water, 842,000 people die from diarrheal disease each year because 2 billion people consume contaminated drinking water sources. Rising water scarcity, population growth, climate change and water delivery systems will continue to face difficulties as a result of urbanization. Additionally, it is predicted that by 2025, the majority of the world's population would reside in regions with water scarcity, where both quantity and quality of water will be compromised, poses a serious threat to human health (15).

Target 6.1 of the Sustainable Development Goals (SDGs) states that everyone should have "equitable access to safe and affordable water". Low-income communities use the sun to disinfect water with the aim of making it safe. This method, also referred to as solar disinfection (SODIS), is cheap and environmentally friendly, and is used to treat water contaminated with *Escherichia coli* (*E.coli*), an enteric bacteria [20], that causes thousands of deaths each year [21], water contaminated with enteric bacteria is usually placed in a transparent plastic bottle, which is exposed to direct sunlight for more than six hours. This inactivates the enteric bacteria, present in the water. However, Bisphenol A, a synthetic monomer that is used to manufacture plastics may leach into the water that is being disinfected [13], making this method relatively unsafe for water disinfection. This compound is considered an endocrine disrupter [6]. Other water disinfection methods include ozonation and chlorination. In ozonation, ozone is able to kill bacteria and pathogenic bacteria that may be persistent in chlorination [11]. However, ozone has one disadvantage, it has low solubility in water and is relatively unstable making it a poor disinfectant in aqueous solution. Chlorination on the other hand, though affordable, it is not effective in eliminating all bacteria and additionally produces toxic byproducts that are mutagenic and carcinogenic even at low concentrations [2] may not be very suitable for disinfection.

To safeguard human health, alternative methods that require disinfection of microorganisms in contaminated water systems have been investigated. Currently, a lot of attention is focused on photo-catalysis. This method uses advanced oxidation technology. When light and semi-conductors interact, highly reactive oxygen radicals like  $\text{OH}^\bullet$ ,  $\text{O}_2^\bullet$ , and  $\text{HO}_2^\bullet$  are produced. These radicals will destroy chemical and biological water contaminants [2].

Bactericidal activity of titanium (IV) oxide,  $\text{TiO}_2$ , as a photo-catalyst has been investigated.  $\text{TiO}_2$  is considered an ideal semiconductor for photo-catalysis because it is highly stable, cheap and relatively safe towards man and the environment [9]. It is an effective semiconductor due its strong oxidising power, when illuminated with UV light at ambient temperatures. Numerous microorganisms, including bacteria, fungus, algae, viruses, and cancerous cells, were discovered to be effectively rendered inactive by  $\text{TiO}_2$  photocatalysts [7]. Studies indicate that when bacteria are exposed to radiation in the presence of  $\text{TiO}_2$ , the cell wall undergoes peroxidation, resulting in leakage of intracellular  $\text{K}^+$  ions [8].

When UV irradiation was removed from water that had been disinfected by UV irradiation, bacteria began to proliferate again [23]. This calls for finding alternative methods that will

completely disinfect contaminated water while generating environmentally safe by-products.  $\text{TiO}_2$  has been modified by researchers to create photocatalysts that are driven by visible light. These modifications include coupling with another semiconductor or a non-metal, doping with an ion, and metal deposition [17]. This will circumvent the challenge of a large band gap and draws the photocatalytic activity into the broad visible light region. Selection of tungsten trioxide and molybdenum trioxide which are narrow band-gap semiconductors (NBS) that function in the visible light region [3], will allow the formation of a heterojunction that shifts the photo response of  $\text{TiO}_2$  from UV to the wide visible light spectrum [26].

In this study, we coupled titanium dioxide with tungsten trioxide to form  $\text{TiO}_2\text{-WO}_3$  nanocomposite and molybdenum trioxide to form  $\text{TiO}_2\text{-MoO}_3$  nanocomposite. They were then characterized using a scanning Electron Microscope (SEM), Transmission Electron Microscope (TEM), and Energy Dispersive X-ray (EDX). *E. coli* was used as a model microbial contaminant for investigating the photocatalytic activity of  $\text{TiO}_2\text{-WO}_3$  and  $\text{TiO}_2\text{-MoO}_3$  nanocomposite under visible light, solar simulator and direct sunlight.

## **2. Materials and Methods**

### **2.1 Chemicals and reagents**

Analytical reagent-grade chemicals were used,  $\text{TiO}_2$  and  $\text{WO}_3$  were bought from Aldrich in South Africa, with purity percentages of 99.4% and 99.995%, respectively. NaF was purchased from Thomas Baker Chemicals in Bharat Mahal, India. Isopropanol from J.T. Baker had a percentage purity of 99.9%. Nitric acid from Uni-CHEM chemical reagents had a purity level of 65%. Agar Agar powder and TM Media EMB Agar were purchased from Scielab in Nairobi. The analytical lab in the Department of Chemistry at the University of Nairobi was where deionized water was obtained.

### **2.2 $\text{TiO}_2$ nanocomposites preparation**

A novel method was used to prepare the photocatalysts at room temperature. 40 ml.  $\text{TiO}_2$ ,  $\text{WO}_3$ , and NaF were weighed out and put in a 1:1:2 molar ratio to isopropanol. Nitric acid was used to keep the mixture at pH of 2, and it was magnetically agitated for 12 hours while exposed to visible light. The precipitate was vacuum-filtered using 0.45  $\mu\text{m}$  membrane filter sheets, cleaned with distilled water, and then dried at 110  $^\circ\text{C}$  in the oven for 12 hours. The product was then calcined for two hours at 575  $^\circ\text{C}$  in a muffle furnace. The procedure was repeated using  $\text{MoO}_3$  in place of  $\text{WO}_3$ .

### **2.3. Characterization of Photocatalysts**

#### **2.3.1. Morphological Analysis**

The nanostructures of  $\text{TiO}_2\text{-WO}_3$  and  $\text{TiO}_2\text{-MoO}_3$  nanocomposite were observed under the Scanning Electron Microscope (SEM) coupled with energy dispersive x-ray (EDX) and the Transmission Electron Microscope (TEM). Characterisation by SEM-EDX involved placing a sample of the photocatalyst on a carbon tape using a small spatula. The tape was mounted on a SEM stub and brought to a low pressure vacuum (LPV) environment using a low vacuum variable pressure secondary electron detector for SEM-EDX analysis (Zeiss Evo LS 15 SEM). Using a high vacuum secondary electron detector, high resolution SEM images were produced. The sample was covered

***Titanium Dioxide Coupled with Tungsten Trioxide and Titanium Dioxide Coupled with Molybdenum Trioxide Nanocomposite-Assisted Photocatalytic Inactivation of Escherichia coli in Direct Sunlight, Solar Simulator, and Visible Light***

with a thin carbon/gold layer using a sputter coater. The purpose of allowing conductivity was to reduce charge between the sample and electron beam. Using a wood splint, two coats of colloidal graphite solution were applied to the carbon tape surrounding the SEM stub. The coating process then took five minutes using a Quorum Coater machine (Q150R ES) in an argon environment. Characterisation by TEM involved filling an Eppendorf tube halfway with a dispersant (deionised water or ethanol). A small amount of the nanocomposite was added, and it was then sonicated on a sonicator for 10 to 15 minutes (Soniclean-Dawe Instruments Ltd., London, England). A grid was carefully placed into the sample solution using tweezers or forceps, then moved onto a fresh piece of Whatman filter paper and allowed to dry after the Eppendorf tube had stood for 30 seconds. The Selected Area Electron Diffraction (SAED) technique was used to analyze TEM micrographs, particle sizes, crystal structures, and diffraction patterns of the nanocomposite [1]. All this was achieved using the TEM (JEOL JEM-1400) equipment.

#### **2.4 Experimental Procedure Sourcing Model Contaminant, Escherichia coli**

*E. coli* was sourced from Kirichwa Ndogo, a part of the Nairobi River that passes through Chiromo campus. EMB Agar, which is a selective media that is enriched to suppress the growth of all the other micro-organisms except the bacteria of interest (*E. coli*) was used as the nutrient. 1  $\mu$ L of water sourced from Kirichwa Ndogo was spread on EMB Agar using a sterile spread rod, and incubated for 24 hours. Thereafter, one colony *E. coli* was taken, placed in 50ml of sterile distilled water and stirred. The concentration of *E. coli* was determined by measuring the absorbance of 1 ml solution at 600nm using a UV-Vis spectrophotometer, followed by conversion of absorbance to colony forming units using an optical density calculator.

##### **2.4.1 Preparation of EMB Agar**

In the EMB Agar preparation, 37.25 g of agar were suspended in 1000 ml of distilled water and heated to boiling to completely dissolve the media. It was then autoclaved for 15 minutes at 121 °C to disinfect it.

##### **2.4.2 Preparation and disinfection of homogenate using TiO<sub>2</sub>-WO<sub>3</sub> and TiO<sub>2</sub>-MoO<sub>3</sub>**

One *E. coli* colony that had been cultivated in the EMB for 24 hours was added to 50 ml of sterile distilled water and agitated for 30 minutes; then 0.05 g of coupled TiO<sub>2</sub>-WO<sub>3</sub> photocatalyst was added while stirring to get a homogenate. The homogenate was exposed to 3 different sources of light: direct sunlight for 6 hours, solar simulator and visible light irradiation sourced from 8W white lamp from Phillips for 3 hours. Using a CYAN pipette, 1 ml of the homogenate was taken every 30 minutes, transferred to a mini centrifuge tube, and centrifuged for 5 minutes at 2000 rpm. 0.1  $\mu$ L of the supernatant liquid was taken and spread on the EMB Agar using a sterile spread rod. The inoculation plates were incubated for 24 hours at a temperature of 37 °C in an incubator. To determine the colony forming units, the colonies that emerged were counted and calculated (cfu). The experiment was repeated using a homogenate that does not have any photocatalyst, this was to study the effect of photolysis under the 3 sources of light.

The profile of sunlight intensity was monitored using a pyranometer (Delta Ohm CE HD2302, Italy) lightmeter connected to a probe irradiance meter (LP471RAD) whose spectral range varied from 400 nm – 1050 nm measuring solar intensity that varied from 0.1 mW m<sup>-2</sup> – 2000W m<sup>-2</sup>. For sunlight, the intensity was recorded every 15 minutes although aliquots of the solution were withdrawn every 30 minutes. The solar intensity for the solar illuminator was set at 1000 Wm<sup>-2</sup> to mimic sun intensity at midday.

The experiments were carried out in triplicate. The effect of different catalyst loading (0.5g/L, 1g/L, 2g/L & 3g/L) was also investigated using coupled TiO<sub>2</sub>-WO<sub>3</sub> only. Figure 1 depicts the experimental setup for rendering *E. coli* inert under visible light set at a distance of 4 cm.

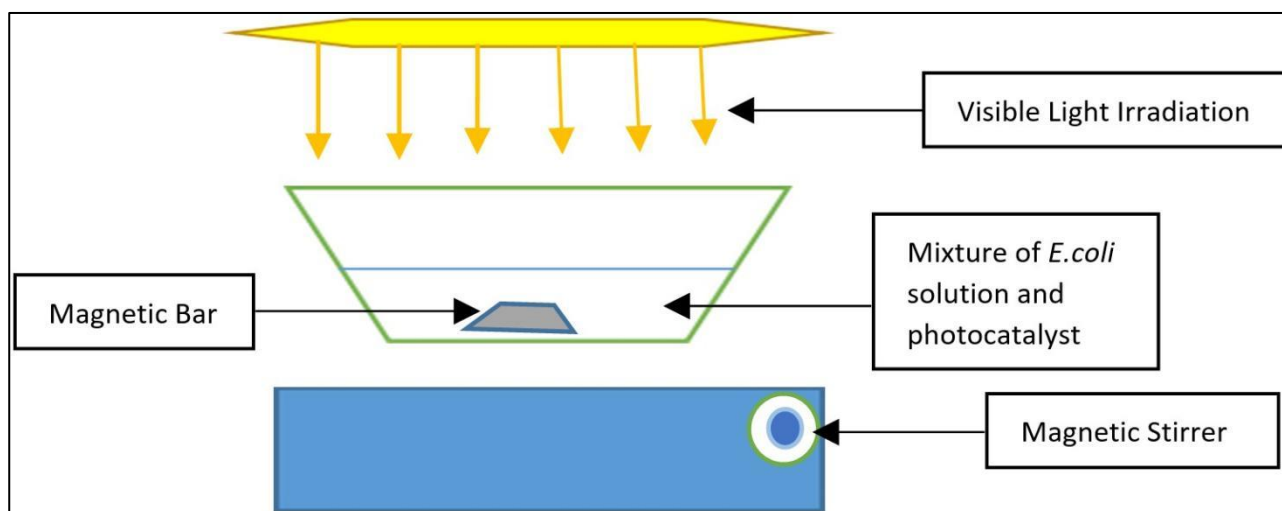


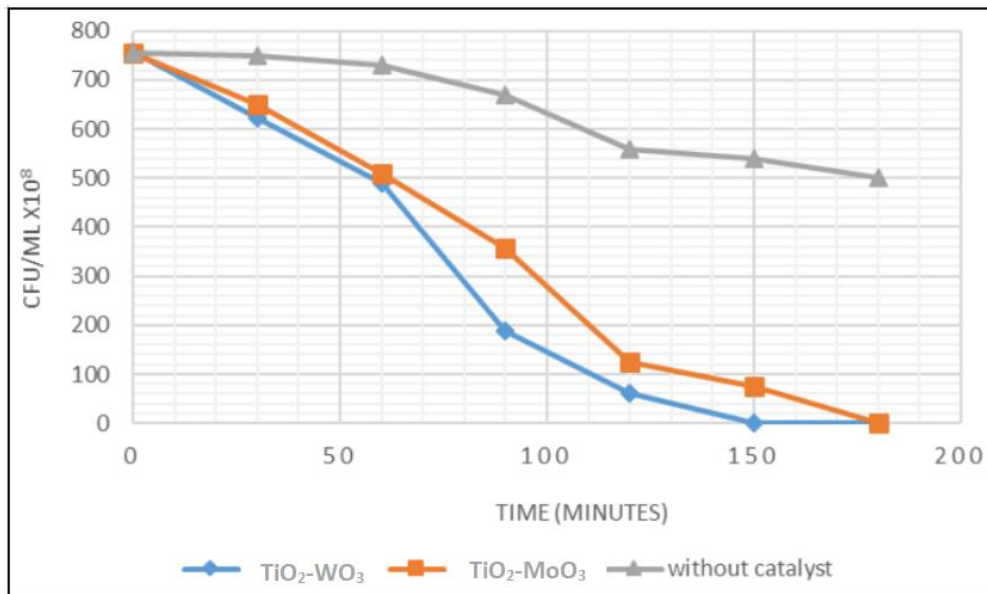
**Figure 1:** Disinfection of escherichia coli using a photocatalyst

### 3 Results and Discussion

#### 3.1 Photocatalytic *E. coli* disinfection under Different Sources of Light

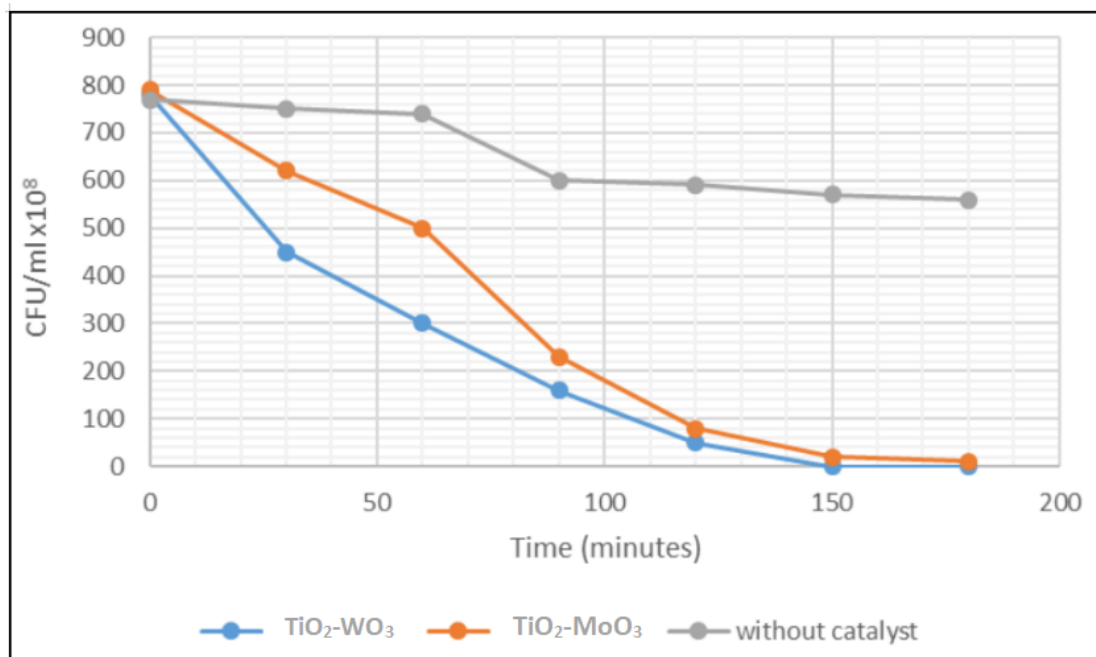
Figures 2, 3, and 4 show the results of photocatalytic disinfection of *E. coli* utilizing TiO<sub>2</sub>-WO<sub>3</sub> and TiO<sub>2</sub>-MoO<sub>3</sub> nanocomposite under various light sources. In each experiment, there was a blank where *E. coli* was exposed to light but in the absence of a photocatalyst. Figure 2 shows a plot of disinfection of *E. coli* under the illumination of a solar simulator. *E. coli* concentration levels drastically reduce for both photocatalysts, indicating that their oxidative stress system has been overwhelmed by the elevated reactive oxygen species levels leading to the disinfection of *E. coli*.

**Titanium Dioxide Coupled with Tungsten Trioxide and Titanium Dioxide Coupled with Molybdenum Trioxide Nanocomposite-Assisted Photocatalytic Inactivation of *Escherichia coli* in Direct Sunlight, Solar Simulator, and Visible Light**



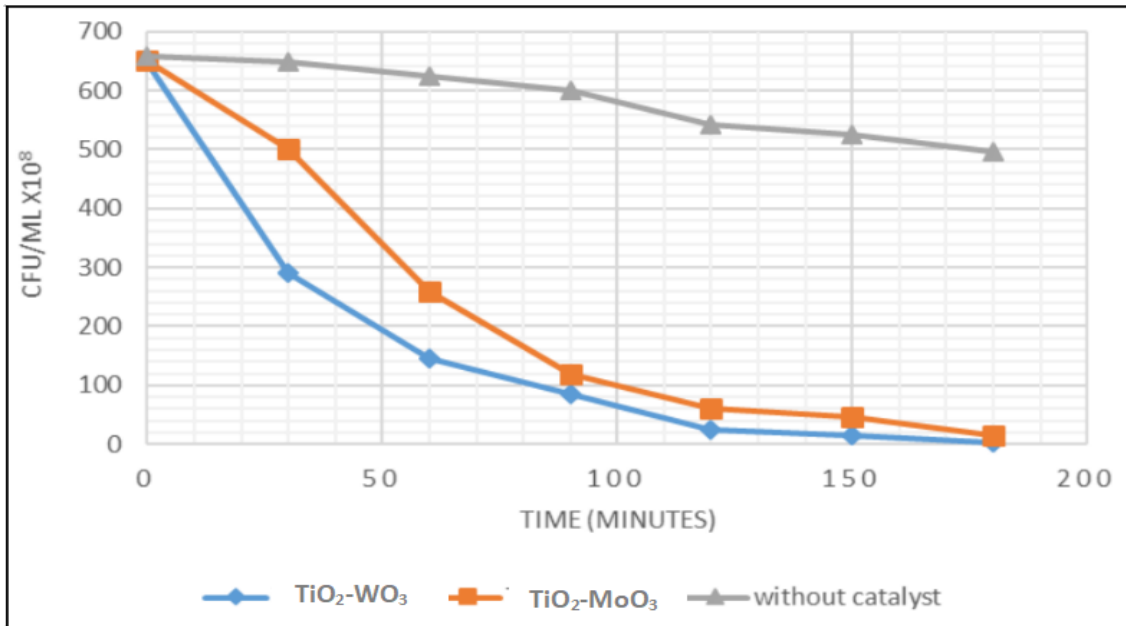
**Figure 2:** *Escherichia coli* inactivation using the Solar Simulator in the presence of 1g/L titanium dioxide coupled with tungsten trioxide and 1g/L titanium dioxide coupled with molybdenum trioxide.

Figure 3 illustrates the disinfection efficacy under visible light. TiO<sub>2</sub>-WO<sub>3</sub> achieves disinfection much quicker than TiO<sub>2</sub>-MoO<sub>3</sub>, finishing in 150 minutes compared to 180 minutes for TiO<sub>2</sub>-MoO<sub>3</sub>.



**Figure 3:** Titanium dioxide coupled with tungsten trioxide and titanium dioxide coupled with molybdenum trioxide nanocomposite-based inactivation of *Escherichia coli* under visible Light using 1g/L of each nanocomposite

Figure 4 depicts disinfection of *E. coli* under natural sunlight. In the first 30 minutes, there was a rapid decrease in *E. coli* levels, indicating that TiO<sub>2</sub>-WO<sub>3</sub> was more effective in deactivating *E. coli* under the prevailing experimental conditions.



**Figure 4:** Escherichia coli inactivation using 1g/L of titanium dioxide coupled with tungsten trioxide and 1g/L of titanium dioxide coupled with molybdenum trioxide nanocomposite under sunlight

In the three blank experiments under different sources of light, *E. coli* levels decreased gradually with time. This clarification emphasizes that besides the photocatalysts, the presence of oxygen in the water interacted with different light sources producing superoxide anion radicals that may have played the role in reducing *E. coli* levels during the experiments.

### 3.2 *E. coli* disinfection utilizing visible light and the impact of photocatalyst loading

Figure 5 shows a plot of coliform forming units (CFU) versus time in minutes, using different catalyst loading.

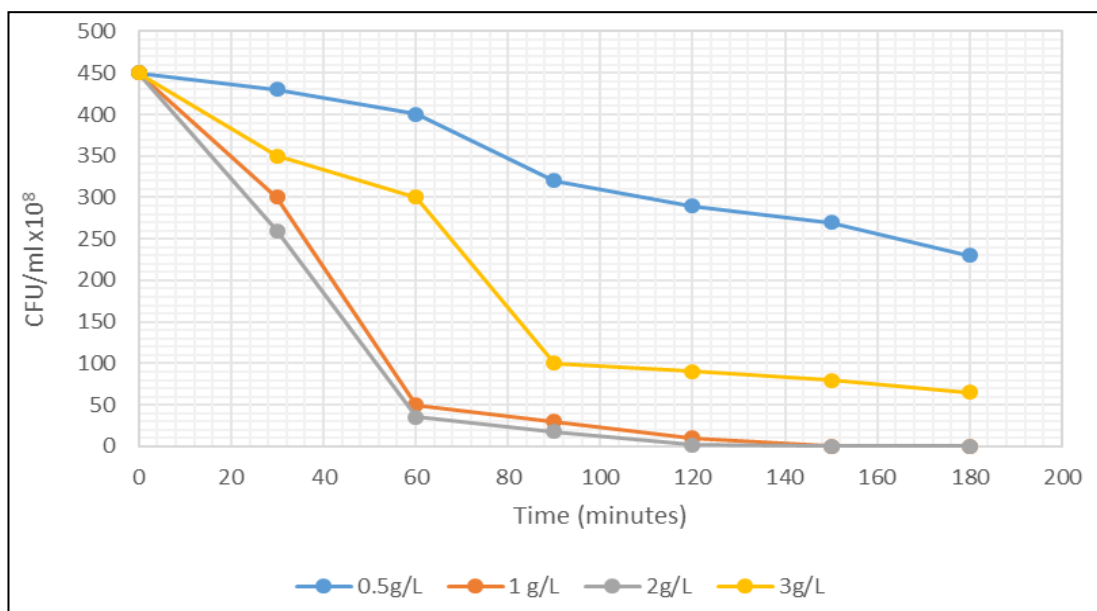


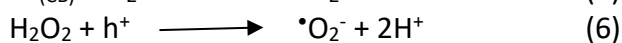
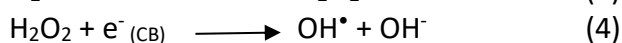
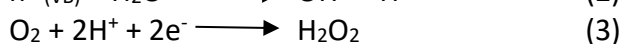
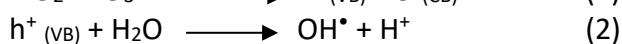
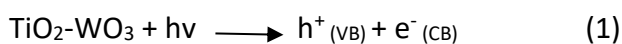
**Figure 5:** Impact of catalyst loading on disinfection of Escherichia coli.

***Titanium Dioxide Coupled with Tungsten Trioxide and Titanium Dioxide Coupled with Molybdenum Trioxide Nanocomposite-Assisted Photocatalytic Inactivation of Escherichia coli in Direct Sunlight, Solar Simulator, and Visible Light***

An essential factor is catalyst loading; when catalyst concentration increases, the disinfection rate also increases. This means a greater surface area is accessible for *E. coli* to adsorb on, facilitating photocatalytic disinfection. The loading will reach a limit, beyond which rate of disinfection will decrease. In this study, the optimal catalyst concentration was 2 g/L and beyond this concentration, the rate of disinfection decreases. The reduction in the rate of disinfection observed above this concentration can be attributed to turbidity that hinders absorption of light radiation. Turbidity results in less ROSs produced which would, therefore be less effective in disinfecting the *E. coli*. Alternatively, the stress defense system in *E. coli* may produce excess intercellular enzymes which will protect *E. coli* by converting the ROS radicals into products that cannot disinfect *E. coli* [19], hence the relatively high values of colony forming units with 3g/L of TiO<sub>2</sub>-WO<sub>3</sub> photocatalyst

### **3.3 Mechanism of photocatalytic *E. coli* disinfection**

This is a photo-oxidative process that involves production of reactive oxygen species (ROS), hydrogen peroxide (H<sub>2</sub>O<sub>2</sub>), the superoxide radical (<sup>•</sup>O<sub>2</sub><sup>-</sup>), and the hydroxyl radical (OH<sup>•</sup>). A photocatalytic technique is used to generate the ROS. A photocatalyst will absorb light photons when exposed to artificial or natural light [26]. A positive hole will form (h<sup>+</sup><sub>VB</sub>) in the valence band and electrons (e<sup>-</sup><sub>CB</sub>) in the conduction band if the energy of the photons of light is equal to or greater than the band gap of the photocatalyst. The hydroxyl radical will be created when the positive hole oxidizes the water on the valence band through a process known as photo-oxidation. The superoxide anion radical will be formed once oxygen gas has been adsorbed on the conduction band, and it can then be transformed to hydrogen peroxide [27]. The entire mechanism that produces ROS is illustrated in equations (1-6) and diagrammatically in figure 6.



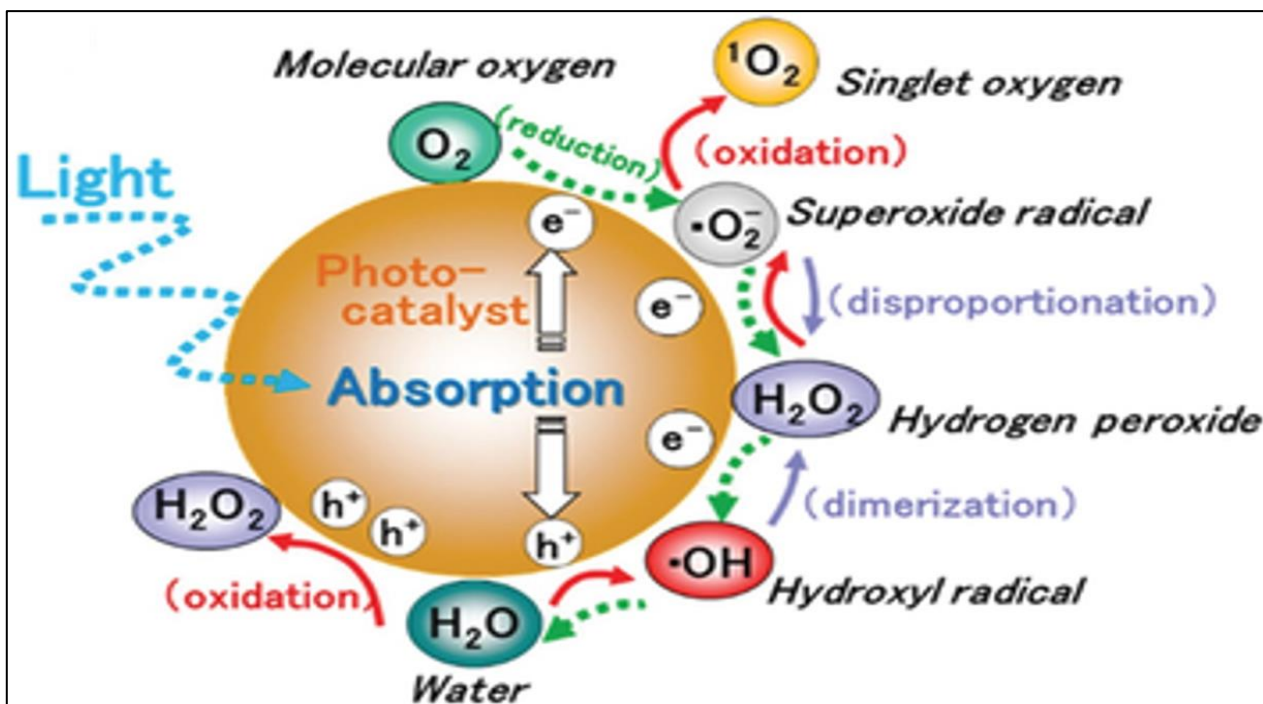


**Figure 6:** Production of reactive oxygen species:  $\text{H}_2\text{O}_2$ ,  $\cdot\text{O}_2^-$  and  $\text{OH}\cdot$ [16]

Studying the redox potentials of the various reactive oxygen species (shown in Table 1), allows one to compare their oxidizing potentials.

**Table 1:** Redox potentials of selected reactive oxygen species [22]

Redox couple	Redox potential, $E^\ominus/\text{V}$
$\text{O}_2/\cdot\text{O}_2^-$	-0.16
$\cdot\text{O}_2^-/\text{H}_2\text{O}_2$	+0.89
$\text{H}_2\text{O}/\text{OH}\cdot$	+2.32
$\text{O}_2/\text{H}_2\text{O}_2$	+0.28

The strongest oxidising agent is the hydroxyl radical, since it has the highest oxidation potential compared to other ROSs. This suggests that hydroxyl radicals are crucial in the disinfection of *E. coli*. Research carried out confirms that the hydroxyl radicals are the main species in *E. coli* disinfection [10]. While lipid peroxidation is a process by which hydroxyl radicals penetrate cell walls and oxidise the membrane fatty acids by extracting an electron from the lipids in the membrane [4], [22]. The cell membrane is harmed as a result of a free radical chain reaction to the cell membrane, proteins and DNA. The superoxide anion radical being negatively charged is not able to penetrate the *E. coli* cell wall, but will oxidise the cell contents.

In contrast, bacterial cells have internal enzymes that shield them from oxidative damage [5], [18]. These are superoxide dismutase (SOD) and catalase (CAT). While the latter is a metalloenzyme that catalyzes the dismutation of the  $\text{O}_2^-$  into hydrogen peroxide and oxygen, the former is an antioxidant enzyme that catalyzes the breakdown of hydrogen peroxide ( $\text{H}_2\text{O}_2$ ) to oxygen and water [12]. If levels of CAT and SOD are high, bacterial cells will remain protected. This implies that the ROS available will be converted into less harmful substances that are unable to attack the *E. coli*. However, if ROS levels exceed levels of CAT and SOD produced by the bacteria, then the cell

**Titanium Dioxide Coupled with Tungsten Trioxide and Titanium Dioxide Coupled with Molybdenum Trioxide Nanocomposite-Assisted Photocatalytic Inactivation of *Escherichia coli* in Direct Sunlight, Solar Simulator, and Visible Light**

membrane of the bacteria will be damaged, causing its destruction and leakage of cell contents. The disinfection of *E. coli* by ROS is illustrated diagrammatically in Figure 7.

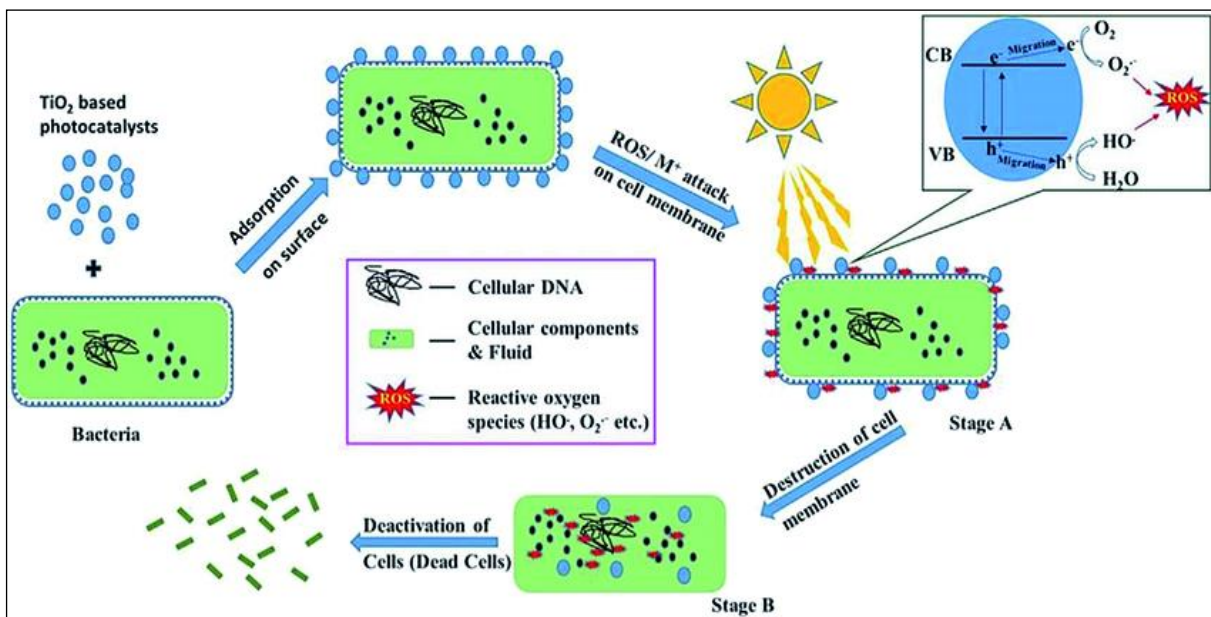


**Figure 7:** Schematic diagram illustrating disinfection of *Escherichia coli* [14]

**3.4. Characterisation using Transmission Electron Microscope**

Figures 8a and 8b illustrate the Transmission Electron Microscopy (TEM) of  $\text{TiO}_2\text{-WO}_3$  and the selected area electron diffraction (SAED) pattern obtained when an electron beam is projected onto a specimen of  $\text{TiO}_2\text{-WO}_3$ . The morphology of  $\text{TiO}_2\text{-WO}_3$  shows irregular spheres with particles of different diameter sizes ranging from 58.66 nm - 143.80 nm. Selected Area Electron Diffraction (SAED) pattern of  $\text{TiO}_2\text{-WO}_3$  shows brightness and spots of a polymorphic ring that is weak. However, the presence of bright spots indicates that the nanocomposite of  $\text{TiO}_2\text{-WO}_3$  is crystalline.

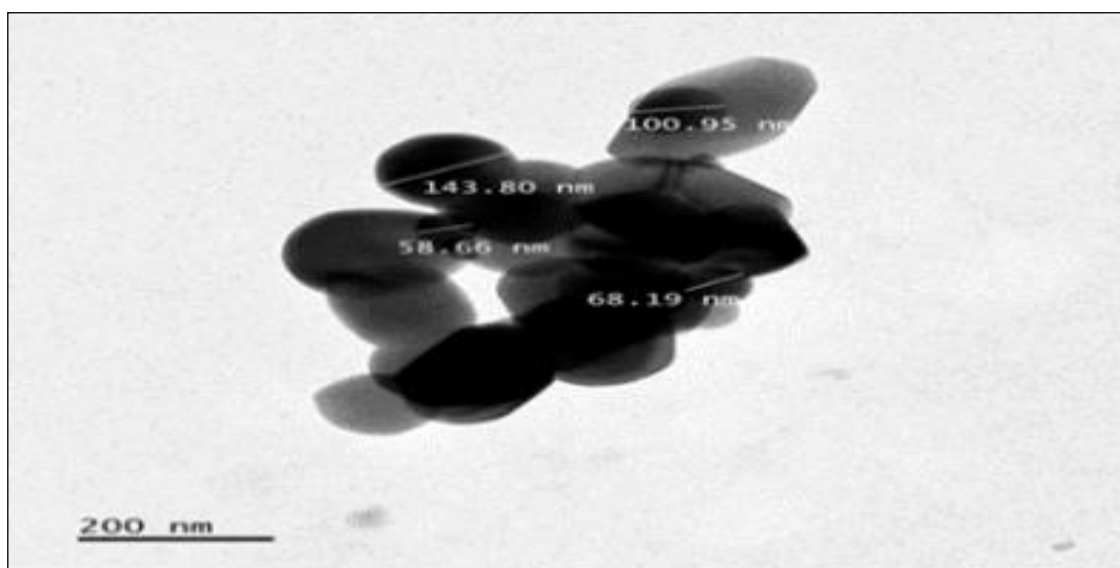


**Figure 8a:** Transmission electron microscopy of titanium dioxide coupled with tungsten trioxide) nanocomposite

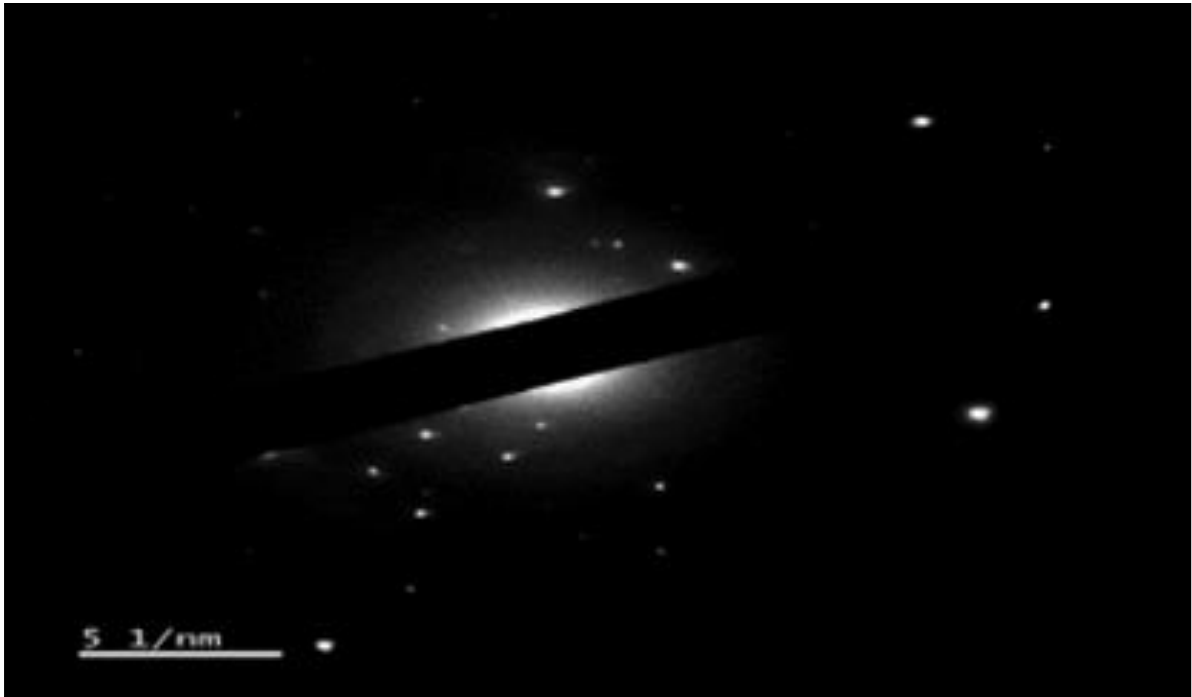


**Figure 8b:** Selected Area Electron Diffraction pattern image of coupled Titanium dioxide coupled with tungsten trioxide) nanocomposite

The Transmission Electron Microscopy of  $\text{TiO}_2\text{-MoO}_3$  is shown in Figure 8c, while its selected area electron diffraction (SAED) pattern is indicated in Figure 8d. The TEM image of  $\text{TiO}_2\text{-MoO}_3$  nanocomposites is composed of spheres with diameters ranging from 67.36 nm - 150.79 nm. The SAED pattern lacks a well-defined ring pattern indicating that it is not polynanocrystalline [1]. The bright spots indicate that it is crystalline.

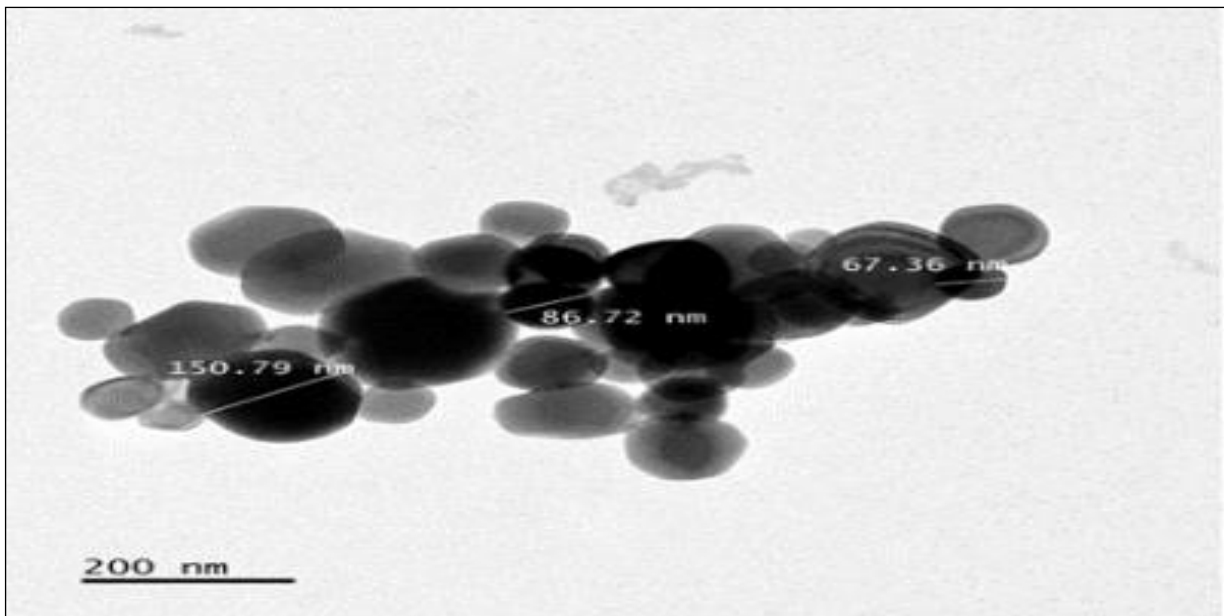


**Figure 8c:** Transmission electron microscopy image of titanium dioxide coupled with molybdenum trioxide nanocomposite

*Titanium Dioxide Coupled with Tungsten Trioxide and Titanium Dioxide Coupled with Molybdenum Trioxide Nanocomposite-Assisted Photocatalytic Inactivation of Escherichia coli in Direct Sunlight, Solar Simulator, and Visible Light*



**Figure 8d:** Selected Area Electron Diffraction pattern image of coupled titanium dioxide coupled with molybdenum trioxide nanocomposite

### 3.5. Energy Dispersive X-ray - Scanning Electron Microscope

Images and energy dispersive X-ray spectra of the nanocomposite materials  $\text{TiO}_2\text{-WO}_3$  and  $\text{TiO}_2\text{-MoO}_3$  are shown in Figures 9a and 9b. The SEM image of  $\text{TiO}_2\text{-WO}_3$  show grain sizes that are approximately uniform with big pores and voids on the surface while the image for  $\text{TiO}_2\text{-MoO}_3$  reveals sheet like structures of different grain sizes with pores that vary in sizes.

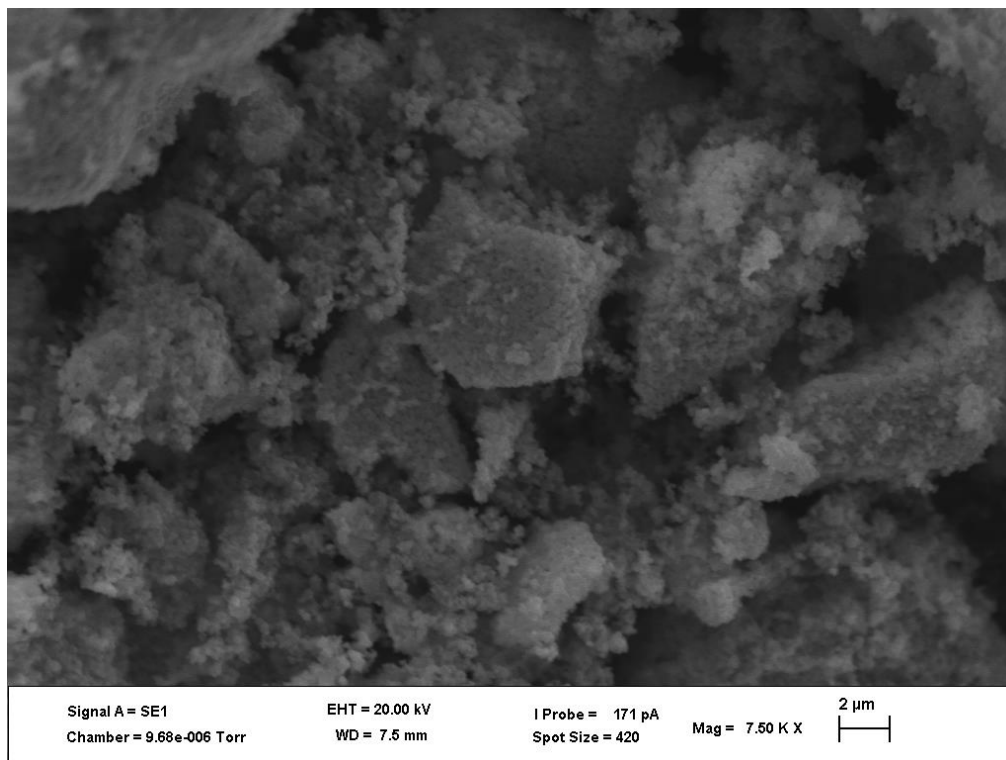


**Figure 9a:** Scanning electron microscope micrograph of coupled titanium dioxide coupled with tungsten trioxide Photocatalyst

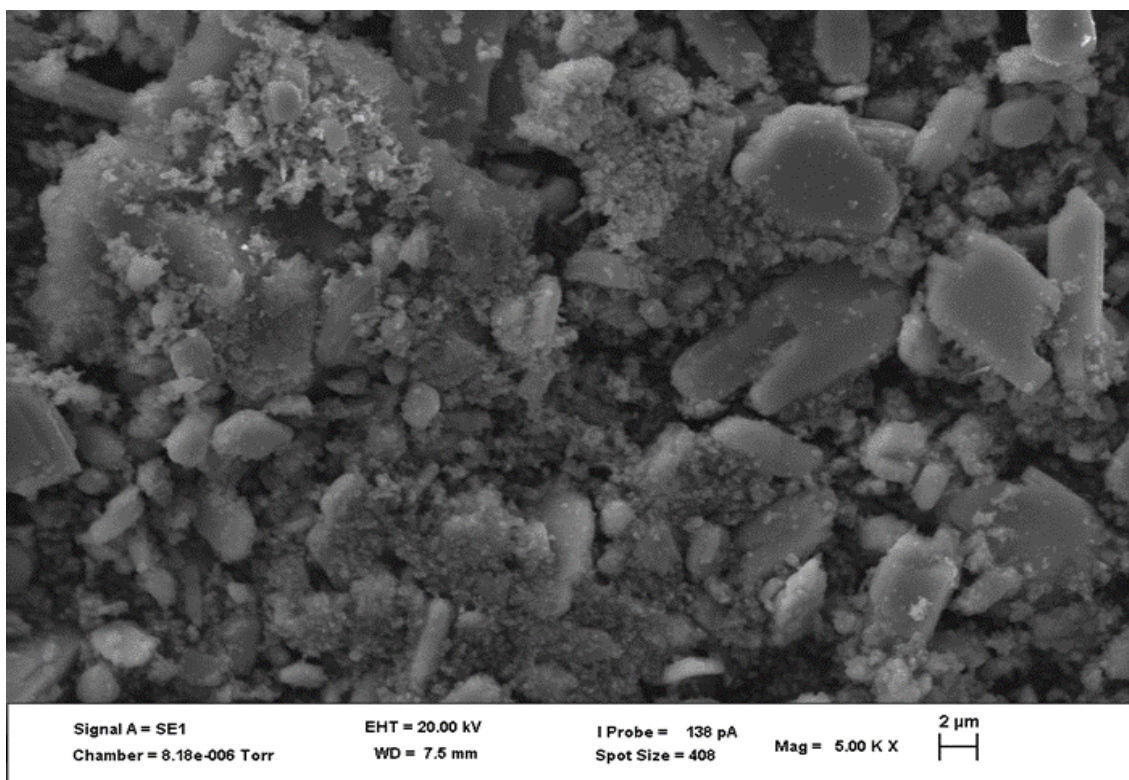


**Figure 9b:** Scanning electron microscope micrograph of coupled titanium dioxide coupled with molybdenum trioxide photocatalyst

The production of  $\text{TiO}_2\text{-WO}_3$  and  $\text{TiO}_2\text{-MoO}_3$  nanoparticles (NPs) was verified by EDX analysis. The equivalent peaks shown in figures 10a and 10b were obtained after various locations were concentrated during measurement. The spectrum for figure 10a, reveals peaks of Ti, W, O and C whose quantities are: 14.94%, 1.49%, 47.71% and 35.86% respectively, while the spectrum for Figure 10b revealed peaks for Ti, Mo, O and C with quantities of: were 8.57%, 5.95%, 50.71% and 34.77%. Values for each element were measured in atomic %. The peaks show strong signals of the main elements present and a weak signal of carbon, they also confirm the formation of coupled  $\text{TiO}_2\text{-WO}_3$  and  $\text{TiO}_2\text{-MoO}_3$  nanocomposite. A carbon peak was observed in each spectra, possible sources EDX of carbon may be the carbon tape, the graphite colloidal solution used in SEM analysis or even the air.

Details of the EDX spectra for the two photocatalysts is recorded in Table 2. The results show % values of chemical composition of each element compared with the theoretical values of their weights.

**Titanium Dioxide Coupled with Tungsten Trioxide and Titanium Dioxide Coupled with Molybdenum Trioxide Nanocomposite-Assisted Photocatalytic Inactivation of Escherichia coli in Direct Sunlight, Solar Simulator, and Visible Light**

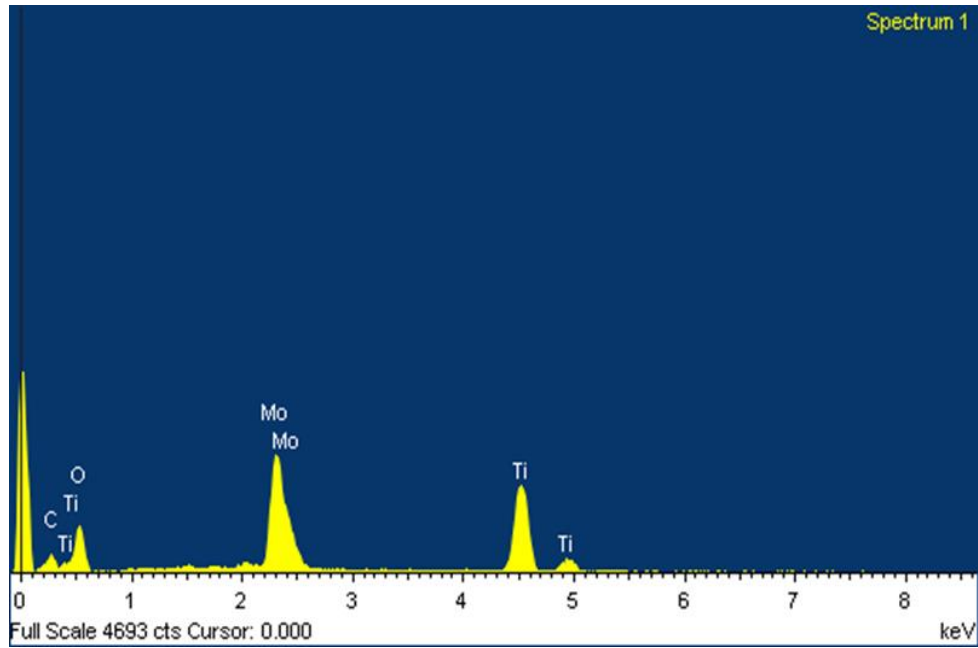


**Figure 10a:** Energy dispersive X-ray spectrum of titanium dioxide coupled with molybdenum trioxide

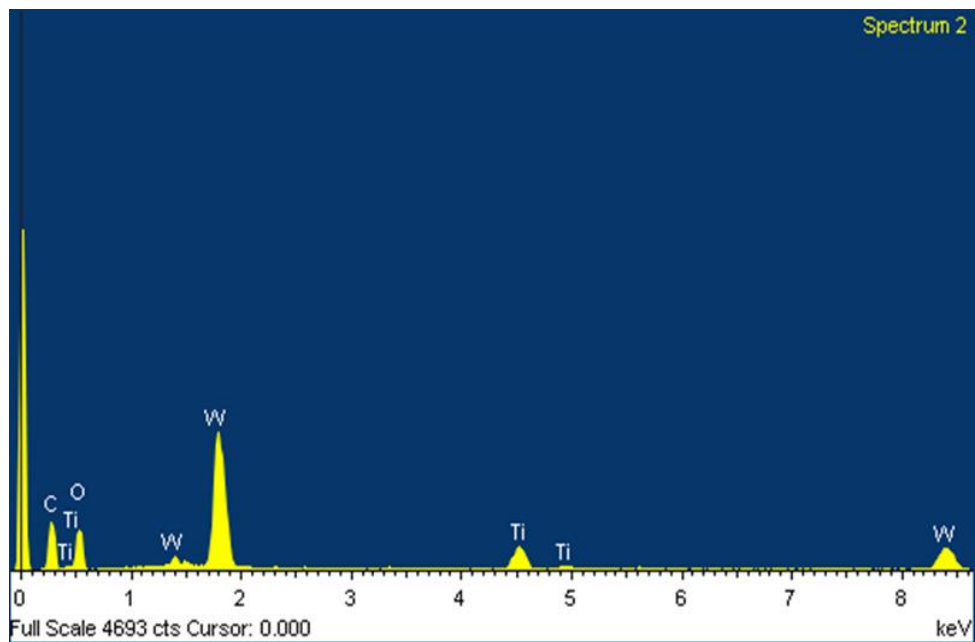


**Figure 10b:** Energy dispersive X-ray spectrum of titanium dioxide coupled with tungsten trioxide

**Table 2:** Elemental composition of Energy dispersive X-ray spectrum of titanium dioxide coupled with tungsten trioxide and titanium dioxide coupled with molybdenum trioxide photocatalysts

<b>TiO<sub>2</sub>-WO<sub>3</sub></b>			<b>TiO<sub>2</sub>-MoO<sub>3</sub></b>		
<b>Element</b>	<b>Weight %</b>	<b>Atomic %</b>	<b>Element</b>	<b>Weight %</b>	<b>Atomic %</b>
C	19.73	35.86	C	18.90	34.77
O	34.97	47.71	O	36.71	50.71
Ti	32.79	14.94	Ti	18.58	8.57
W	12.52	1.49	Mo	25.82	5.95
Totals	100.00		Totals	100.00	

## Conclusion

In this study, two coupled photocatalysts, TiO<sub>2</sub>-WO<sub>3</sub> and TiO<sub>2</sub>-MoO<sub>3</sub>, were tested for photocatalytic disinfection of *Escherichia coli* (*E. coli*) using visible light, sunlight, and a solar simulator over a three-hour period. Results showed that TiO<sub>2</sub>-WO<sub>3</sub> was more effective against gram-negative *E. coli* compared to TiO<sub>2</sub>-MoO<sub>3</sub> across all light sources. Disinfection results after 60 minutes of irradiation indicated under direct sunlight, TiO<sub>2</sub>-WO<sub>3</sub> achieved 78% disinfection and TiO<sub>2</sub>-MoO<sub>3</sub> achieved 66%, while under visible light, TiO<sub>2</sub>-WO<sub>3</sub> achieved 64% and TiO<sub>2</sub>-MoO<sub>3</sub> achieved 33%. Solar simulator illumination showed 35% disinfection for TiO<sub>2</sub>-WO<sub>3</sub> and 32% for TiO<sub>2</sub>-MoO<sub>3</sub>. Both visible light and solar simulator provided stable artificial radiation distinct from sunlight, promoting charge separation, increased charge carriers, and reactive oxygen species production, crucial for *E. coli* disinfection. Notably, disinfection rates under sunlight were particularly promising, suggesting intermittent sunlight exposure contributes significantly to *E. coli* inactivation. This study underscores photocatalysis as a promising advanced oxidation process for *E. coli* disinfection, potentially offering an alternative to chlorination in water treatment pending further practical research.

## Disclosure statement

No conflicts of interest are disclosed by the authors.

## Acknowledgements

DAAD and NRF provided funding for this study.

## References

- [1] Asadabad, M. A., & Eskandari, M. J. (2016). Electron Diffraction. In M. Janecek & R. Kral (Eds.), *Modern Electron Microscopy in Physical and Life Sciences*. InTech. <https://doi.org/10.5772/61781>
- [2] Benabbou, A. K., Derriche, Z., Felix, C., Lejeune, P., & Guillard, C. (2007). Photocatalytic inactivation of *Escherichia coli*. *Applied Catalysis B: Environmental*, 76(3–4), 257–263. <https://doi.org/10.1016/j.apcatb.2007.05.026>
- [3] Bera, S., Won, D.-I., Rawal, S. B., Kang, H. J., & Lee, W. I. (2019). Design of visible-light photocatalysts by coupling of inorganic semiconductors. *Catalysis Today*, 335, 3–19. <https://doi.org/10.1016/j.cattod.2018.11.001>
- [4] Bogdan, J., Zarzyńska, J., & Pławińska-Czarnak, J. (2015). Comparison of Infectious Agents Susceptibility to Photocatalytic Effects of Nanosized Titanium and Zinc Oxides: A Practical Approach. *Nanoscale Research Letters*, 10(1). <https://doi.org/10.1186/s11671-015-1023-z>
- [5] Cheng, J.-H., Lv, X., Pan, Y., & Sun, D.-W. (2020). Foodborne bacterial stress responses to exogenous reactive oxygen species (ROS) induced by cold plasma treatments. *Trends in Food Science & Technology*, 103, 239–247. <https://doi.org/10.1016/j.tifs.2020.07.022>
- [6] Dominguez, S., Huebra, M., Han, C., Campo, P., Nadagouda, M. N., Rivero, M. J., Ortiz, I., & Dionysiou, D. D. (2017). Magnetically recoverable TiO<sub>2</sub>-WO<sub>3</sub> photocatalyst to oxidize bisphenol A from model wastewater under simulated solar light. *Environmental Science and Pollution Research*, 24(14), 12589–12598. <https://doi.org/10.1007/s11356-016-7564-6>
- [7] Foster, H. A., Ditta, I. B., Varghese, S., & Steele, A. (2011). Photocatalytic disinfection using titanium dioxide: Spectrum and mechanism of antimicrobial activity. *Applied Microbiology and Biotechnology*, 90(6), 1847–1868. <https://doi.org/10.1007/s00253-011-3213-7>
- [8] Ganguly, P., Byrne, C., Breen, A., & Pillai, S. C. (2018). Antimicrobial activity of photocatalysts: Fundamentals, mechanisms, kinetics and recent advances. *Applied Catalysis B: Environmental*, 225, 51–75. <https://doi.org/10.1016/j.apcatb.2017.11.018>
- [9] Gupta, S. M., & Tripathi, M. (2011). A review of TiO<sub>2</sub> nanoparticles. *Chinese Science Bulletin*, 56(16), 1639–1657. <https://doi.org/10.1007/s11434-011-4476-1>
- [10] Jeong, J., Kim, C., & Yoon, J. (2009). The effect of electrode material on the generation of oxidants and microbial inactivation in the electrochemical disinfection processes. *Water Research*, 43(4), 895–901. <https://doi.org/10.1016/j.watres.2008.11.033>

**Titanium Dioxide Coupled with Tungsten Trioxide and Titanium Dioxide Coupled with Molybdenum Trioxide Nanocomposite-Assisted Photocatalytic Inactivation of Escherichia coli in Direct Sunlight, Solar Simulator, and Visible Light**

- [11] Karamah, E. F., & Sunarko, I. (2013). Disinfection of Bacteria Escherichia Coli using Hydrodynamic Cavitation. *International Journal of Technology*, 4(3), 209. <https://doi.org/10.14716/ijtech.v4i3.116>
- [12] Kashmiri, Z. N., & Mankar, S. A. (2014). Free radicals and oxidative stress in bacteria. *International Journal of Current Microbiology and Applied Sciences*, 3(9), 34-40.
- [13] Kiio, K. L., Mbui, D., Michira, I., & Njenga, H. Analysis of Bisphenol A in drinking water bottles and baby feeding bottles using Polyaniline/Bentonite Modified Glassy Carbon Electrode Biosensor. *Journal of Applied Chemistry*, 12(4), 1-11
- [14] Laxma Reddy, P. V., Kavitha, B., Kumar Reddy, P. A., & Kim, K.-H. (2017). TiO<sub>2</sub>-based photocatalytic disinfection of microbes in aqueous media: A review. *Environmental Research*, 154, 296–303. <https://doi.org/10.1016/j.envres.2017.01.018>
- [15] Mulwa, F., Li, Z., & Fangninou, F. F. (2021). Water scarcity in Kenya: current status, challenges and future solutions. *Open Access Library Journal*, 8(1), 1-15.
- [16] Nosaka, Y., & Nosaka, A. Y. (2017). Generation and Detection of Reactive Oxygen Species in Photocatalysis. *Chemical Reviews*, 117(17), 11302–11336. <https://doi.org/10.1021/acs.chemrev.7b00161>
- [17] Pawar, M., Topcu Sendoğdular, S., & Gouma, P. (2018). A Brief Overview of TiO<sub>2</sub> Photocatalyst for Organic Dye Remediation: Case Study of Reaction Mechanisms Involved in Ce-TiO<sub>2</sub> Photocatalysts System. *Journal of Nanomaterials*, 2018, 1–13. <https://doi.org/10.1155/2018/5953609>
- [18] Sharma, P., Jha, A. B., Dubey, R. S., & Pessarakli, M. (2012). Reactive Oxygen Species, Oxidative Damage, and Antioxidative Defense Mechanism in Plants under Stressful Conditions. *Journal of Botany*, 2012, 1–26. <https://doi.org/10.1155/2012/217037>
- [18] Suzuki, J., Imamura, M., Nakano, D., Yamamoto, R., & Fujita, M. (2018). Effects of water turbidity and different temperatures on oxidative stress in caddisfly (*Stenopsyche marmorata*) larvae. *Science of the total environment*, 630, 1078-1085.
- [19] Ubomba-Jaswa, E., Boyle, M., & Mcguigan, K. (2008). Inactivation of enteropathogenic *E. coli* by solar disinfection (SODIS) under simulated sunlight conditions. *Journal of Physics: Conference Series*, 101. <https://doi.org/10.1088/1742-6596/101/1/012003>
- [20] Varnagiris, Š., Urbonavicius, M., Sakalauskaitė, S., Daugelavicius, R., Pranevicius, L., Lelis, M., & Milcius, D. (2020). Floating TiO<sub>2</sub> photocatalyst for efficient inactivation of *E. coli* and decomposition of methylene blue solution. *Science of the Total Environment*, 720, 137600. <https://doi.org/10.1016/j.scitotenv.2020.137600>
- [21] Vatansever, F., de Melo, W. C. M. A., Avci, P., Vecchio, D., Sadasivam, M., Gupta, A., Chandran, R., Karimi, M., Parizotto, N. A., Yin, R., Tegos, G. P., & Hamblin, M. R. (2013). Antimicrobial strategies centered around reactive oxygen species – bactericidal antibiotics, photodynamic therapy, and beyond. *FEMS Microbiology Reviews*, 37(6), 955–989. <https://doi.org/10.1111/1574-6976.12026>
- [22] Wang, W., Huang, G., Yu, J. C., & Wong, P. K. (2015). Advances in photocatalytic disinfection of bacteria: Development of photocatalysts and mechanisms. *Journal of Environmental Sciences*, 34, 232–247. <https://doi.org/10.1016/j.jes.2015.05.003>
- [23] WHO, (2022). *Drinking-water*. Retrieved March 29, 2022, from <https://www.who.int/news-room/fact-sheets/detail/drinking-water>
- [24] Yang, C., Dong, W., Cui, G., Zhao, Y., Shi, X., Xia, X., Tang, B., & Wang, W. (2017). Highly-efficient photocatalytic degradation of methylene blue by PoPD-modified TiO<sub>2</sub> nanocomposites due to photosensitization-synergetic effect of TiO<sub>2</sub> with PoPD. *Scientific Reports*, 7(1), 3973. <https://doi.org/10.1038/s41598-017-04398-x>
- [25] Žerjav, G., Arshad, M. S., Djinović, P., Junkar, I., Kovač, J., Zavašnik, J., & Pintar, A. (2017). Improved electron–hole separation and migration in anatase TiO<sub>2</sub> nanorod/reduced graphene oxide composites and their influence on photocatalytic performance. *Nanoscale*, 9(13), 4578-4592.
- [26] Zhang, L., Qin, M., Yu, W., Zhang, Q., Xie, H., Sun, Z., Shao, Q., Guo, X., Hao, L., Zheng, Y., & Guo, Z. (2017). Heterostructured TiO<sub>2</sub> /WO<sub>3</sub> Nanocomposites for Photocatalytic Degradation of Toluene under Visible Light. *Journal of the Electrochemical Society*, 164(14), H1086–H1090. <https://doi.org/10.1149/2.0881714jes>